

Article

An Envelope-to-Cycle Difference Compensation Method for eLoran Signals in Seawater Based on a Variable Step Size Least Mean Square Algorithm

Miao Wu ¹ , Liang Liu ¹ , Fangneng Li ^{1,*}, Bing Zhu ², Wenkui Li ¹ and Xianzhou Jin ¹

¹ The College of Electrical Engineering, Naval University of Engineering, Wuhan 430033, China; wumiao2652@163.com (M.W.); brilliancy909@163.com (L.L.); li_wenkui123@163.com (W.L.); jxz2065629079@163.com (X.J.)

² Beijing Institute of Tracking and Communication Technology, Beijing 100000, China; zhubingtqq@163.com

* Correspondence: fangneng_li@126.com

Abstract: The dispersion effect of seawater can cause the envelop distortion of underwater eLoran signals, which causes the envelope-to-cycle difference (ECD) to exceed the standard range. Furthermore, it results in incorrect cycle identification and significant positioning errors. However, few studies have focused on the distortion caused by the dispersion effect. In this study, we propose an accurate underwater eLoran ECD compensation method based on a variable step size least mean square (VSS-LMS) algorithm. First, a systematic modeling approach was employed to investigate the impact of dispersion effects on Loran signals. Second, the VSS-LMS algorithm was introduced to update the filter weight vector in response to discrepancies in the input signal. Finally, the input signal was subjected to an adaptive transversal filtering process, resulting in an output signal that adhered to the specifications of the ECD standard. The efficacy and superiority of the proposed algorithm were demonstrated by experimentation and simulation. When the depth of seawater exceeds 2 m, the ECD value of the original eLoran signal exceeds the standard range, precluding the possibility of cycle identification. However, when the depth of seawater reaches 4 m, the ECD of the signal compensated by the proposed algorithm adaptively compensates for the normal range, thereby enabling the accurate recognition of cycles.

Keywords: eLoran; envelope-to-cycle difference (ECD); variable step size least mean square algorithm (VSS-LMS); dispersion effect; cyclic identification



Academic Editor: Arturo de la Escalera Hueso

Received: 24 December 2024

Revised: 24 January 2025

Accepted: 29 January 2025

Published: 3 February 2025

Citation: Wu, M.; Liu, L.; Li, F.; Zhu, B.; Li, W.; Jin, X. An Envelope-to-Cycle Difference Compensation Method for eLoran Signals in Seawater Based on a Variable Step Size Least Mean Square Algorithm. *Electronics* **2025**, *14*, 597. <https://doi.org/10.3390/electronics14030597>

Copyright: © 2025 by the authors. Licensee MDPI, Basel, Switzerland. This article is an open access article distributed under the terms and conditions of the Creative Commons Attribution (CC BY) license (<https://creativecommons.org/licenses/by/4.0/>).

1. Introduction

The global navigation satellite system (GNSS) has been the subject of considerable interest due to its high positioning accuracy, extensive coverage, and straightforward usability [1]. However, the system's inherent frequency characteristics render it unsuitable for utilization in marine environments. The Loran-C system is a land-based radio navigation system with good stability, anti-interference ability, and excellent positioning ability. A novel iteration of the Loran-C system, eLoran, is regarded as a viable contingency for the GNSS, with a positioning accuracy of up to 20 m in specific contexts [2,3]. The eLoran system operates in the low-frequency band at 90 kHz to 110 kHz. It can facilitate navigation in shallow waters, thereby superseding the functionality of the GNSS in seawater. Seawater is a dispersive medium, and eLoran signals exhibit disparate phase velocities at each frequency within the seawater medium. This phenomenon gives rise to deviations in the signal envelope. The Loran system is a double-curve positioning system that utilizes the

signal's third-cycle positive zero-crossing point time information. Detecting the third-cycle positive zero-crossing point is crucial for positioning accuracy. The difference between the received signal envelope and the standard signal envelope is 1%, resulting in a difference of 0.6 μs in the zero-crossing point and a deviation of 180 m in positioning accuracy [4].

To provide accurate positioning, navigation, and timing (PNT) services for underwater equipment in the vast and complex marine environment, the development of underwater navigation technology is necessary to promote the development of aquatic resources, the maintenance of national security, and the detection of the marine environment [5]. The eLoran system is a long-wave radio navigation system with a more substantial in-water capability than satellite radio signals. It can provide better PNT services for underwater users without requiring the user's equipment to surface to improve its stealth. In recent years, Korea has begun to deploy the new eLoran system to provide reliable PNT services for users up to 30 km off the coast [6]. It has already started to create ASF databases for some narrow waterways to provide more accurate positioning services [7].

In recent years, many researchers have attempted to employ the eLoran system in marine environments. In reference [8], electromagnetic propagation analysis and experimental verification proved that a magnetic antenna can be used to receive the Roland C signal in a seawater environment. In reference [9], the influence of seawater dispersion on the Loran-C signal was analyzed by creating an accurate seawater propagation model. It was concluded that seawater dispersion causes the pulse front to broaden and the third-cycle zero-crossing time to advance. The above scholars have not yet discussed and analyzed the abnormal envelope-to-cycle difference (ECD) values caused by the underwater dispersion effect. The pulse-signal broadening distorts the signal envelope, resulting in abnormal ECD values. The system is not able to identify the period accurately. To use the eLoran system in a seawater environment, research on the abnormal ECD values in a seawater environment and a discussion regarding compensation methods are required.

The least mean square (LMS) algorithm proposed by Widrow and Hoff [10] has been employed in many fields, such as noise suppression [11,12], echo cancellation [13], magnetic field compensation [14], and channel equalization [15]. The basis of the LMS algorithm is that the transversal filter coefficients are adjusted using the difference between the input signal and the desired signal. First, a transversal filter is initialized, and an appropriate step factor is selected. Next, the algorithmically processed output is computed based on the current filter coefficients and the input signal. Then, the error signal is determined by comparing this output to the desired signal. Finally, the filter coefficients are updated using a linear combination of the error signal and the learning rate. This process is iterated until the error converges, ensuring optimized filter performance. Kwong et al. proposed a variable step size least mean square (VSS-LMS) algorithm that optimizes the performance of the traditional LMS algorithm by adjusting the step-size parameter according to the error [16]. The proposed algorithm allows the step size to be dynamically adjusted with the magnitude of the error during the operation. In the early stages of the algorithm, a more significant step size is used to ensure rapid convergence. As the algorithm progresses, the step size is gradually reduced to reduce steady-state error and improve signal-processing accuracy. This approach enhances the algorithm's convergence speed while improving its performance under steady-state conditions. Due to the uncertainty of the underwater environment, an adaptive filtering algorithm is employed to obtain the ideal signal by adjusting the filter weights. In the eLoran system, the initial 65 μs of information from the pulse signal are utilized, ensuring the adaptation filter complies with requirements. In this scenario, the VSS-LMS algorithm, as an adaptive algorithm, can meet these requirements by adaptively adjusting the step-size parameter according to the varying stages of the signal, thereby ensuring both rapid convergence and effective oscillation attenuation.

The present paper proposes using the VSS-LMS algorithm to address the abnormal eLoran signal ECD caused by the dispersion effect of seawater. Section 2 models the sea-water dispersion effect of eLoran. The signal distortion at different seawater depths and the numerical value of the ECD are explained using simulation experiments. A VSS-LMS-based underwater dispersion processing method is proposed for abnormal ECD conditions. Section 3 employs theoretical calculations to obtain the eLoran signal in a simulated seawater environment. The VSS-LMS algorithm is then utilized to adjust the simulated signal, thereby demonstrating the compensated ECD value. Subsequently, the experiment data verifies the change in underwater ECD and the usability of the VSS-LMS algorithm in a real seawater environment. Section 4 concludes the paper.

2. Analysis of Seawater Propagation and Signal Compensation for eLoran Signals

2.1. The eLoran Seawater Model

In the design of the eLoran signal, it is necessary to ensure that the single pulse waveform exhibits a short pulse rise time, a narrow spectrum, and a small ECD value. Therefore, the envelope of a single eLoran signal pulse is teardrop-shaped, rising sharply to a maximum within the first 65 ms. The standard normalized expression for eLoran signals is as follows:

$$i(t) = \begin{cases} \left(\frac{t-\tau}{65}\right)^2 e^{\left(\frac{-2(t-\tau)}{65}-1\right)} \sin(0.2\pi t + p) & \tau \leq t \leq 65 + \tau \\ 0 & t < \tau \end{cases} \quad (1)$$

where t is the time; the unit is microseconds; τ is the starting point of the envelope time, also known as the envelope period difference; and p is the phase encoding parameter.

In the context of eLoran, the envelope cycle difference refers to the discrepancy between the identification point of the signal envelope and the third positive-cycle zero crossing. When the identification point occurs after the third-cycle zero crossing, the ECD is positive; conversely, when the identification point precedes the third-cycle zero crossing, the ECD is negative [17]. The following Figure 1 shows the eLoran waveform with an ECD of 2 μ s:

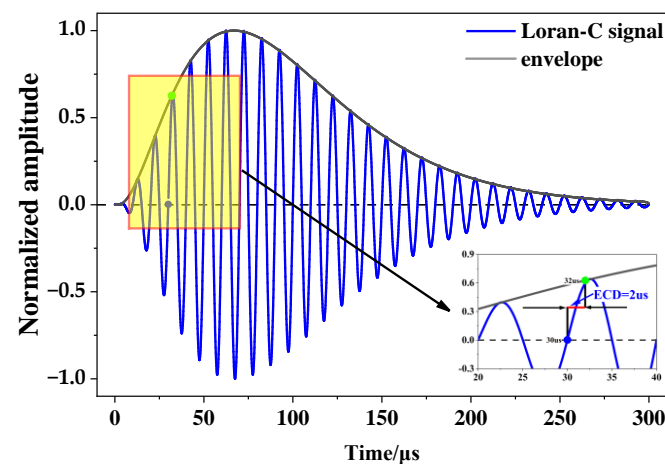


Figure 1. The eLoran waveform with ECD of 2 μ s.

A U.S. Department of Transportation report detailed that the eLoran system is deemed stable when the ECD range falls between -2.4μ s and 2.4μ s. Outside of this specified range, periodic identification is rendered inaccurate [18].

In order to accurately identify the positive over-zero point of the third cycle, the half-cycle peak ratio (HCPR) method is used for the analysis. A standard HCPR threshold

is pre-stored within the receiving device. When the detected HCPR value reaches this threshold, the corresponding point is identified as the feature identification point of the envelope cycle. Subsequently, the positive zero-crossing point immediately adjacent to this identification point is then identified as the positive zero-crossing point of the third cycle. However, if the ECD value exceeds 2.4 μs , there is a risk that the feature identification point may be closer to the fourth cycle than to the expected third cycle. In this case, a misclassification may result, i.e., the positive over-zero point of the fourth cycle is incorrectly identified as the positive over-zero point of the third cycle. To avoid such errors when the receiving device performs cycle identification, the ECD of the eLoran signal needs to be evaluated and signals that exceed the bounds not recognized.

The operating frequency range of the eLoran system signal is 90 kHz–110 kHz. The propagation speed of each frequency is different in seawater, and the phase relationship of the propagated signal changes, distorting the signal envelope and causing the ECD value to increase beyond the standard range. To analyze the dispersion effect of eLoran signals in seawater, it was first necessary to construct a propagation model for electromagnetic waves. This paper employs Maxwell's equations to examine the propagation of electromagnetic waves in dispersive media. The resulting wave equation for electromagnetic wave signals in time-varying fields is presented as follows [19]:

$$\begin{cases} \nabla^2 \times \vec{E} + \omega^2 \mu_0 \epsilon_e \vec{E} = 0 \\ \nabla^2 \times \vec{H} + \omega^2 \mu_0 \epsilon_e \vec{H} = 0 \end{cases} \quad (2)$$

where \vec{E} is the electric field vector excited by the transmitting antenna, \vec{H} is the magnetic field vector, ω is the angular frequency of the transmitted signal, μ_0 is the magnetic permeability of the transmission path, ϵ_e is the complex permittivity of the transmission path, and ∇ is the Hamiltonian function.

When electromagnetic waves propagate deep into the ocean, only the effect of depth on signal strength and phase is considered. This is to say that the field quantity of the electromagnetic field is only related to the Z-axis. Let us consider that the electric field strength \vec{E} and the magnetic field strength \vec{H} can be determined from the electric field source according to the following relationship:

$$\vec{H} = \frac{j}{\omega \mu_0} \nabla \times \vec{E} = \frac{j}{\omega \mu_0} (\nabla E_x) \times e_x \quad (3)$$

where E_x is the electric field component in the X-axis direction, e_x is the unit direction vector, and j is the imaginary unit. It can be obtained because the electric field strength is only related to the Z-axis component.

$$\frac{\partial E_x}{\partial x} = \frac{\partial E_x}{\partial y} = 0 \quad (4)$$

$$\nabla E_x = e_x \frac{\partial E_x}{\partial x} + e_y \frac{\partial E_x}{\partial y} + e_z \frac{\partial E_x}{\partial z} = e_z \frac{\partial E_x}{\partial z} \quad (5)$$

Substituting Equation (5) into Equation (3), it can be simplified as:

$$\vec{H} = e_y \frac{j}{\omega \mu_0} \frac{\partial E_x}{\partial z} = e_y H_y. \quad (6)$$

From Equation (6), it can be seen that the magnetic field strength is solely in the Y component, and it can be seen that the electric field and the magnetic field are perpendicular

to each other. Finally, by substituting the electric field strength and Equation (5) into the time-harmonic electric field Equation (2), we obtain:

$$\frac{d^2 E_x}{dz^2} + k_1^2 E_x = 0. \quad (7)$$

As demonstrated by Equation (7), the second-order differential equation can be solved to yield the following result:

$$E = E_x e^{-jk_1 z} + E'_x e^{jk_1 z}. \quad (8)$$

In Equation (8), the first term represents the direction of the radio wave propagating under seawater, and the second term represents the radio wave propagating upward along the air. What is studied in this paper is the change in the eLoran signal propagating under seawater, so it can be simplified as follows [20]:

$$E = E_x e^{-jk_1 z} \quad (9)$$

$$k_1 = \alpha - j\beta \quad (10)$$

$$\alpha = \omega \sqrt{\frac{\mu_0 \varepsilon}{2} \left(\sqrt{1 + \left(\frac{\sigma}{\omega \varepsilon} \right)^2} + 1 \right)} \quad (11)$$

$$\beta = \omega \sqrt{\frac{\mu_0 \varepsilon}{2} \left(\sqrt{1 + \left(\frac{\sigma}{\omega \varepsilon} \right)^2} - 1 \right)} \quad (12)$$

where α is called the attenuation constant and represents the attenuation of eLoran signal strength in seawater, β is called the phase constant and represents the change in phase seawater of the eLoran signal, σ is the conductivity of the seawater medium, ε is the conductivity of the seawater medium, and z is the depth of the seawater.

Phase velocity refers to the speed of propagation of a phase of an electromagnetic wave through space, which can be obtained from the ratio between the frequency and phase parameters of the electromagnetic wave:

$$V_p = \frac{\omega}{\beta} = \frac{1}{\omega \sqrt{\frac{\mu \varepsilon}{2} \left(\sqrt{1 + \left(\frac{\sigma}{\omega \varepsilon} \right)^2} - 1 \right)}}. \quad (13)$$

Electromagnetic waves of different frequencies propagate at different speeds in the same medium, a phenomenon called dispersion. From Equation (13), it can be observed that the phase velocity is frequency-dependent, and the eLoran signal operates in the frequency band from 90 to 110 kHz. In this frequency range, there is a difference in the phase velocity of electromagnetic waves of different frequencies in water, which means that they propagate at slightly different speeds. Therefore, when these components with different phase velocities arrive at the receiving device, they do not arrive simultaneously but with a time delay. This time difference causes the superimposed effect of the individual frequency components to differ from the original transmitted signal, which in turn distorts the received signal waveform. This affects the accuracy of the resolution and positioning of the signal.

Therefore, the amplitude attenuation $A(k)$ and phase change $B(k)$ in the eLoran at different under seawater depths are:

$$\begin{cases} A(k) = e^{-\alpha z} \\ B(k) = e^{-\beta z} \end{cases}. \quad (14)$$

Given that the loss tangent $\frac{\sigma}{\epsilon\omega} \gg 1$ of electromagnetic waves propagating in water is greater than one and that seawater can be regarded as a good conductor, the phase and attenuation constant are approximately equal. Consequently, Equations (11) and (12) can be simplified as:

$$\alpha = \beta = \sqrt{\frac{\omega\mu\epsilon}{2}}. \tag{15}$$

A discrete Fourier transformation of the standard eLoran signal is as follows:

$$I(k) = \sum_{n=0}^{N-1} i(t)e^{-j(\frac{2\pi}{N})nk} \tag{16}$$

where k is the frequency and N is the sample length of the signal.

The amplitude and phase of the standard signal are calculated in the frequency domain, and the resulting amplitude attenuation and phase change in seawater under each frequency are then superimposed to obtain the following equation:

$$I'(n) = \sum_{k=0}^{N-1} A(k)abs(I(k))e^{(j \cdot \arg(I(k)) - B(k))}. \tag{17}$$

Finally, the Fourier inverse transformation is applied to Equation (17) to restore the time-domain waveform. Subsequently, the waveform's ECD value is calculated and evaluated.

First, the received signal is normalized by comparing the deviation between the actual and standard waveforms of the first eight half-cycle peaks and calculating the root mean square error M as expressed in Equation (18). The T value corresponding to the minimum error is the ECD value of the actual waveform. In practice, the interval for using τ is $-10 \mu\text{s}$ to $10 \mu\text{s}$. Figure 2 shows a flowchart of the ECD calculation of the received signal.

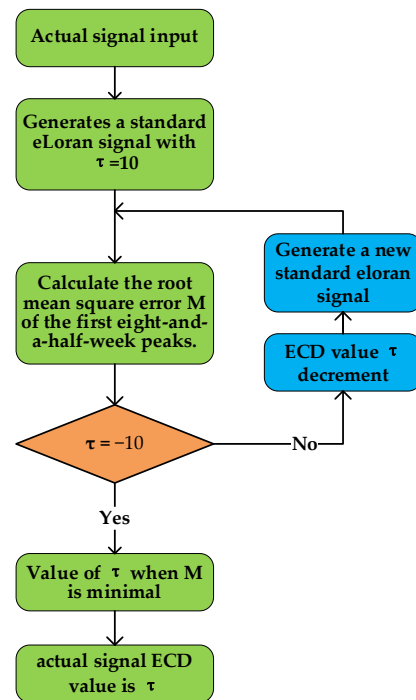


Figure 2. Signal ECD calculation flowchart for eLoran.

$$M = \left[\frac{\sum_{i=1}^8 (I_i - S_i)^2}{8} \right]^{1/2} \tag{18}$$

Here, I_i is the i th half-peak of the standard waveform $ECD = \tau$, and S_i is the n th half-peak of the actual waveform.

According to the above theoretical model, when the conductivity of the seawater medium into which the eLoran signal enters is set to be 4 s/m and the relative dielectric constant is 80, the eLoran signal is calculated in the time-domain waveforms of the eLoran signal at seawater depths of 0–4 m according to Equation (17), as shown in Figure 3. Based on the signal waveform at each depth, the peaks of the first eight half-cycles of the eLoran are found, and the ECD is calculated according to Equation (18) to obtain Table 1.

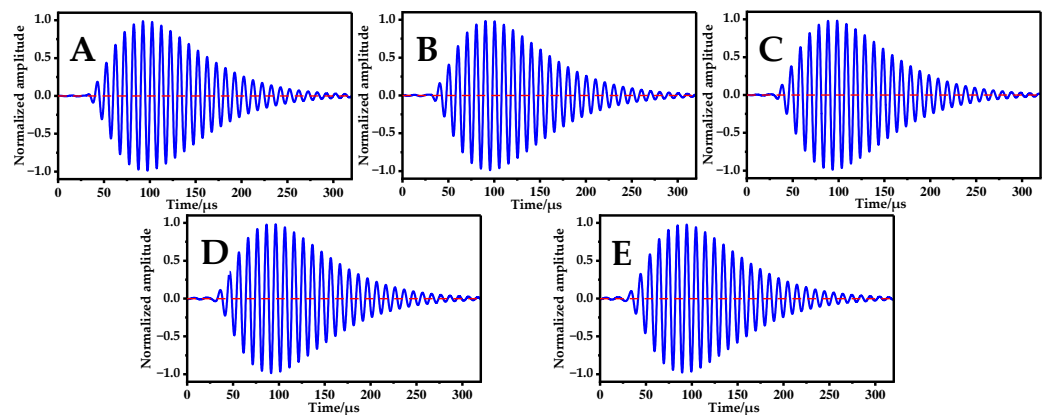


Figure 3. Normalized eLoran signal waveforms at different depths: (A) sea surface, (B) seawater depth 1 m, (C) seawater depth 2 m, (D) seawater depth 3 m, (E) seawater depth 4 m.

Table 1. The first eight half-cycle peaks and ECD at different depths.

Depth \ m	Peak of the First Eight-and-a-Half Cycles								ECD \ μs
	1	2	3	4	5	6	7	8	
0	0.0157	−0.0833	0.1901	−0.3158	0.4454	−0.5696	0.6813	−0.7771	0.00
1	0.0104	−0.0680	0.1614	−0.2790	0.4080	−0.5356	0.6526	−0.7524	1.30
2	0.0104	−0.0498	0.1346	−0.2491	0.3794	−0.5112	0.6326	−0.7360	2.40
3	0.0139	−0.0356	0.1131	−0.2248	0.3547	−0.4875	0.6105	−0.7161	3.40
4	0.0182	−0.0333	0.0970	−0.2001	0.3259	−0.4588	0.5852	−0.6964	4.40

The data presented in Table 1 illustrates that as the depth of the seawater medium increases, the second to eighth half-cycle peaks continue to decrease, increasing the packet cycle difference value. Upon reaching a depth of 2 m, the ECD value surpasses the established threshold, rendering the system incapable of accurately identifying the third-cycle positive zero-point. The simulation above illustrates the impact of seawater dispersion on the eLoran signal.

2.2. Signal Algorithm Compensation of eLoran

The eLoran signal is significantly compromised in seawater, resulting in anomalous ECD values. The VSS-LMS algorithm has been proposed to correct the signal distortion, thereby ensuring that the ECD meets the identification standard of the receiving device. The traditional LMS algorithm minimizes the error of updating the adaptive filter’s weight coefficient to ensure the output signal reaches the desired form. This principle is illus-

trated in Figure 4. The VSS algorithm represents an improvement on the traditional LMS algorithm, as it employs different step sizes for different error values to update the filter's weight coefficient, thereby facilitating rapid error convergence. The VSS_LMS algorithm process is shown in Algorithm 1.

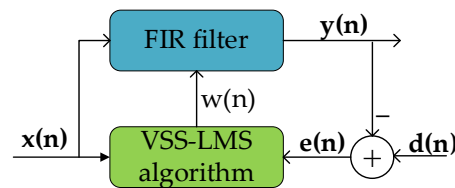


Figure 4. Schematic diagram of VSS-LMS algorithm.

The received eLoran signal $x(n)$ is input into an n th-order transverse filter with a set weight coefficient $w_i(n)$, and the resulting output signal $y(n)$ can be expressed as follows:

$$y(n) = \sum_{i=0}^N w_i(n)x(n-i) = \mathbf{w}^T(n)\mathbf{x}(n). \quad (19)$$

The key component of the VSS-LMS algorithm is the calculation of errors. If we assume that the anticipated response $d(n)$ is a standard eLoran signal, the resulting error $e(n)$ is:

$$e(n) = d(n) - y(n) = d(n) - \mathbf{w}^T(n)\mathbf{x}(n). \quad (20)$$

We then update the filter weight coefficients based on the error:

$$\mathbf{w}(n+1) = \mathbf{w}(n) + \mu(n)\mathbf{x}(n)e(n). \quad (21)$$

The step parameter at time $n+1$ can be updated by utilizing the signal error at time n and the step size:

$$\mu(n+1) = \alpha\mu(n) + \gamma e^2(n) \quad (22)$$

where α and γ are designated as smoothing factors. During experimental procedures, the value of α is typically set to 0.97, while the value of γ is maintained at a level below 4.8×10^{-4} .

Algorithm 1: VSS-LMS algorithmic process

Initialization: $N = 30$, $\alpha = 0.97$, $\gamma = 4.8 \times 10^{-4}$, $\mathbf{w}(0) = [0 \cdots 0]_{1 \times 30}$, $\mu = 1$

While receiving data, do the following

data update:

1. filter output $y(n) \leftarrow \mathbf{x}(n)$
2. output response error calculation $e(n) \leftarrow y(n)$
3. step size update $\mu(n+1) \leftarrow [\mu(n), e(n)]$
4. filter weight vector update $\mathbf{w}(n+1) \leftarrow [\mathbf{w}(n), \mu(n), \mathbf{x}(n), e(n)]$

END

3. The eLoran Underwater Transmission Simulation and Experiment

3.1. The eLoran Under Seawater Simulation

The VSS-LMS algorithm rectified the signal according to varying seawater depths, yielding the waveform data illustrated in Figure 5 and the data in Table 2. A transversal filter structure with a filter coefficient of 50 was utilized. The initial settings for the VSS-LMS algorithm anticipated a standard normalized eLoran signal.

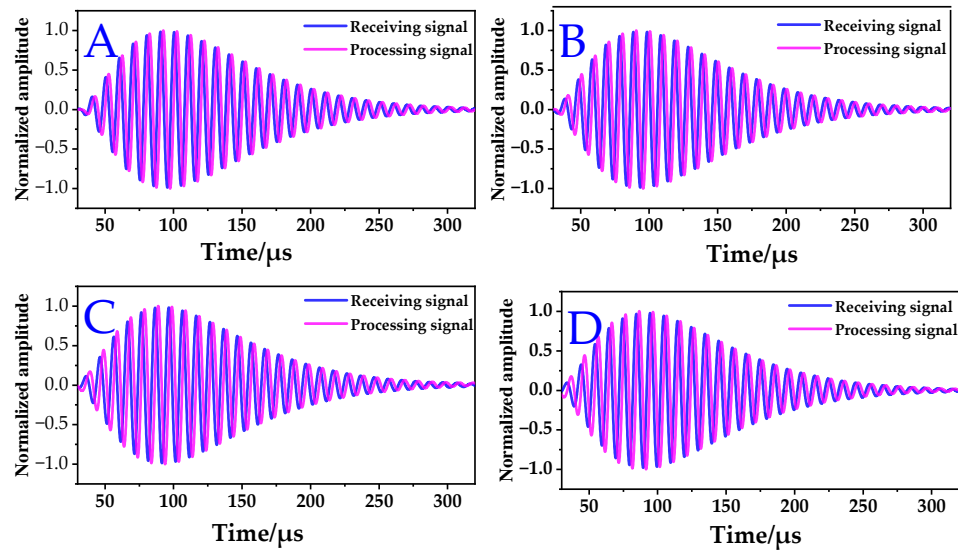


Figure 5. VSS-LMS algorithm correction of eLoran analogue signals at different seawater depths: (A) seawater depth 1 m, (B) seawater depth 2 m, (C) seawater depth 3 m, (D) seawater depth 4 m.

Table 2. The first eight half-cycle peaks of the signal after processing by the VSS-LMS algorithm and ECD at different seawater depths.

Depth \ m	Peak of the First Eight-and-a-Half Cycles								ECD \ μs
	1	2	3	4	5	6	7	8	
1	0.0007	−0.0568	0.1660	−0.3172	0.4482	−0.5698	0.6820	−0.7771	0.30
2	0.0032	−0.0632	0.1787	−0.3174	0.4459	−0.5701	0.6814	−0.7774	0.20
3	0.0129	−0.0709	0.1711	−0.3155	0.4439	−0.5688	0.6812	−0.7764	0.70
4	0.0266	−0.0877	0.1768	−0.3079	0.4437	−0.5677	0.6813	−0.7758	0.80

As illustrated in Table 2, following compensation by the VSS-LMS algorithm, the eLoran signal can be maintained within a stable range of $-2.4 \mu\text{s}$ to $2.4 \mu\text{s}$ within a depth of 4 m of seawater. However, as the signal depth increases, the ECD of the compensated eLoran signal also increases, resulting in a reduction in signal stability. At a seawater depth of 3 m, Table 1 indicates that the uncompensated signal ECD is $3.4 \mu\text{s}$. In contrast, Table 2 demonstrates that the compensated signal ECD is $0.7 \mu\text{s}$, representing an 80% reduction compared to the simulated signal. Figure 5D illustrates that when the depth of the seawater is 4 m, the amplitude of the front end of the pulse increases, and the root mean square error of the first eight half-cycle peaks decreases following the processing of the signal by the VSS-LMS algorithm. This results in a reduction in the ECD value of the eLoran signal. As illustrated in Figure 5 and Table 2, the VSS-LMS algorithm can effectively address signal distortion issues caused by seawater, enabling the signal to be utilized in a seawater environment at a depth of 4 m.

3.2. Experiment

To confirm the alterations in the eLoran signal within seawater, a magnetic antenna and receiver were employed to obtain the 6780-station chain signal at five distinct seawater depths. Figure 6A illustrates the shape of the magnetic antenna. In contrast, Figure 6B–D depict the environment of the magnetic antenna on the sea surface, 1 m below the surface, and 4 m below the surface, respectively. The signal received by the magnetic field antenna was normalized and then corrected using the LMS algorithm, thereby obtaining the signal waveform illustrated in Figure 7. Subsequently, an analysis and calculation were conducted to obtain Table 3.

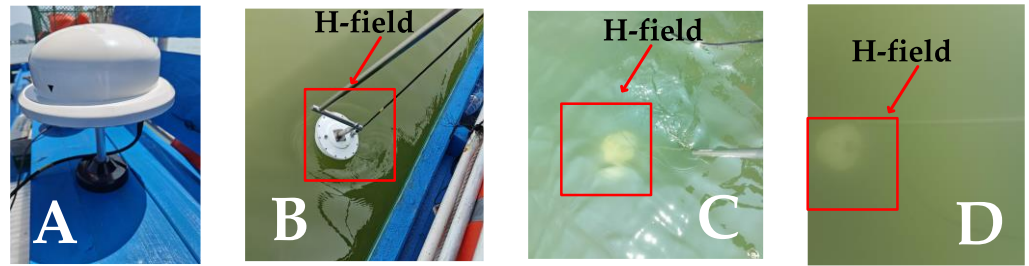


Figure 6. H-field state: (A) magnetic antenna shape, (B) sea surface reception status of magnetic antenna, (C) magnetic antenna 1 m underwater receiving status, (D) magnetic antenna receiving state of 4 m underwater.

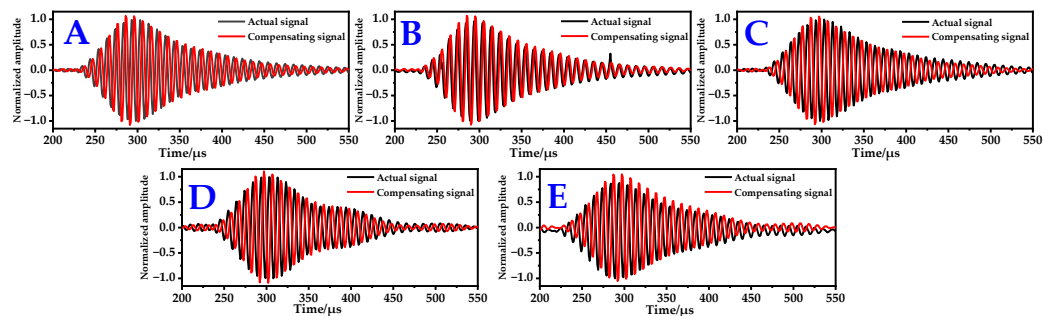


Figure 7. The signal is received at different seawater depths, and the VSS-LMS algorithm compensates for the signal: (A) sea surface, (B) seawater depth 1 m, (C) seawater depth 2 m, (D) seawater depth 3 m, (E) seawater depth 4 m.

Table 3. ECD of the uncompensated signal and compensated signal.

Depth \ m	Uncompensated Signal ECD \ μs	Compensated Signal with Proposed Method ECD \ μs
0	0.40	−0.10
1	1.60	0.70
2	3.50	1.40
3	4.70	1.60
4	5.00	2.20

As illustrated in Table 3, the elevation in the ECD value of the eLoran signal is more pronounced in seawater. When the depth of the seawater surpasses 2 m, the signal ECD reaches 3.5 μs , which exceeds the standard ECD limit. The receiving equipment cannot accurately identify the signal cycle at this depth, resulting in a considerable deviation in positioning accuracy. Table 2 illustrates that, under simulated conditions, the eLoran signal is situated at a depth of 2 m beneath seawater, with an ECD value of 2.5 μs . However, in actual reception, the ECD value is 3.5 μs , representing a 45.8% increase. The seawater conductivity under simulated conditions is less than that observed in actual seawater, which results in a considerable discrepancy in ECD values. The dispersion signal is processed using the VSS-LMS algorithm, compensating for the amplitude. The signal remains within the ECD standard limits within a depth of 4 m in seawater. Before compensation, the ECD is 5 μs ; the ECD is reduced by 56% following signal compensation. The preceding experiment demonstrated that the VSS-LMS algorithm can effectively address the impact of seawater dispersion on the eLoran signal ECD, thereby enhancing the stability of the eLoran signal. This enables the eLoran device to identify the third-week positive zero crossing accurately and improves the navigation capability of the system in marine environments.

4. Conclusions

This paper explores the dispersion effect encountered by eLoran signals when propagating in the marine environment, which leads to a substantial deviation in ECD. A correction method based on the variable step size least mean square algorithm is proposed to effectively address abnormal ECD values. Experimental and simulation results demonstrate that as the depth of seawater increases, the ECD of the eLoran signal tends to increase. When the seawater depth reaches 2 m, the ECD exceeds the set limit, which may lead to periodic identification errors.

The VSS-LMS algorithm corrected the abnormal ECD signal in the test data. The experimental results show that in seawater that is not deeper than 4 m, the compensated signal ECD value remains within the normal range. Considering that the eLoran signal strength drops below the device's reception threshold under more than 4 m of water depth, this experimental scenario aligns more with actual application conditions. The research results show that the VSS-LMS algorithm can effectively correct the eLoran signal ECD anomalies caused by the seawater environment, thereby ensuring the accuracy of cycle identification, improving the reliability and accuracy of the eLoran system, and providing a more accurate time benchmark for underwater navigation.

The existing conditions limited this experiment, and dynamic factors, such as the activities of surrounding vessels and marine weather, have not yet been considered in the experimental results. In future studies, we plan to conduct relevant experiments in more complex environments and under strong interference conditions to further test and optimize the algorithm proposed in this paper. With these improvements, the method is expected to significantly enhance the adaptability and robustness of the eLoran system in complex marine environments, providing important support for the development of underwater navigation technology. Subsequent studies will deeply explore the algorithm's performance under different marine environment parameters and develop corresponding optimization strategies to ensure its effectiveness and reliability in various application scenarios.

Author Contributions: M.W. and L.L. conceived the content and structure of the paper; L.L. Analyzed simulation data and wrote papers; F.L., W.L. and B.Z. helped with discussion and revision; L.L. and X.J. completed the software code to analyze the data. All authors have read and agreed to the published version of the manuscript.

Funding: This work was supported by the National Natural Science Foundation of China, grant number 42174051.

Data Availability Statement: The data will be made available upon request.

Conflicts of Interest: The authors declare no conflicts of interest.

Abbreviations

Acronym	Full Forms
eLoran	Enhanced long-range navigation
PNT	Positioning, navigation, and timing
ECD	Envelope-to-cycle difference
VSS-LMS	Variable step size least mean square
GNSS	Global navigation satellite system
Loran-C	Long-range navigation C
LMS	Least mean square
HCPR	Half-cycle peak ratio

References

1. Chang, S.; Ji, B.; Wu, M.; Bian, S.; Li, W.; Du, H. Evaluation of Height Correction on Loran Signal's Groundwave Transmission Delay Model. *Antennas Wirel. Propag. Lett.* **2023**, *22*, 1005–1009. [[CrossRef](#)]
2. Pelgrum, W. New Potential of Low-Frequency Radionavigation in the 21st Century. Ph.D. Thesis, TU Delft, Delft, The Netherlands, 2006.
3. Wu, M.; Di, J.; Xu, J.; Li, F. Application and development of eLoran. *Hydrogr. Surv. Charting* **2022**, *42*, 44–49. [[CrossRef](#)]
4. Wu, M.; Zhu, Y.; Li, F.; Xu, J. *Radio Navigation Principle and Signal Receiving Technology*; National Defense Industry Press: Beijing, China, 2015; ISBN 978-7-118-09795-5.
5. Bian, H.; Xu, J.; He, H.; Ma, H.; Wang, R. Information Architecture and Key Issues of Underwater PNT System. *Navig. Position. Timing* **2022**, *9*, 31–39. [[CrossRef](#)]
6. Son, P.-W.; Park, S.G.; Han, Y.; Seo, K. eLoran: Resilient Positioning, Navigation, and Timing Infrastructure in Maritime Areas. *IEEE Access* **2020**, *8*, 193708–193716. [[CrossRef](#)]
7. Kim, W.; Son, P.-W.; Park, S.G.; Park, S.H.; Seo, J. First Demonstration of the Korean eLoran Accuracy in a Narrow Waterway Using Improved ASF Maps. *IEEE Trans. Aerosp. Electron. Syst.* **2022**, *58*, 1492–1496. [[CrossRef](#)]
8. Cui, G.; Xu, J.; Cao, K.; Zhu, Y. Research on Feasibility of Receiving Loran-C Signal Underwater with H-Field Antenna. In Proceedings of the 2010 2nd International Conference on Signal Processing Systems, Dalian, China, 5–7 July 2010; Volume 2, pp. V2-678–V2-681.
9. Zhou, L.; Mu, Z.; Pu, Y.; Xi, X.; He, L. Study on the Prediction Theory and Algorithm of Loran-C Signals Propagation Characteristics Under Water. *Acta Electron.* **2017**, *45*, 1206–1210. [[CrossRef](#)]
10. Widrow, B.; McCool, J.M.; Larimore, M.G.; Johnson, C.R. Stationary and Nonstationary Learning Characteristics of the LMS Adaptive Filter. *Proc. IEEE* **1976**, *64*, 1151–1162. [[CrossRef](#)]
11. Prasad, N.; Prakash, D.; Dixit, S. Implementation of Optimized Adaptive LMS Noise Cancellation System to Enhance Signal to Noise Ratio. In Proceedings of the 2023 2nd International Conference on Applied Artificial Intelligence and Computing (ICAIC), Salem, India, 4–6 May 2023; pp. 1581–1586.
12. Zhang, H.; Li, J.; Cheng, Y.; Liu, F.; Qu, C. Adaptive Denoising Study Based on Improved Variable Step Size LMS Algorithm. In Proceedings of the 2024 Second International Conference on Cyber-Energy Systems and Intelligent Energy (ICCSIE), Shenyang, China, 17–19 May 2024; pp. 1–6.
13. Reddy, V.K.V.; Kavya, Y.; Prasad, P.; Krishna, K.B.; Harika, D. Enhanced VLSI Speech Enhancement Systems Utilizing Adaptive LMS Filters and Machine Learning Techniques for Echo Cancellation. In Proceedings of the 2024 International Conference on Intelligent Systems for Cybersecurity (ISCS), Gurugram, India, 3–4 May 2024; pp. 1–6.
14. Ponikvar, D.; Zupanič, E.; Jeglič, P. Magnetic Interference Compensation Using the Adaptive LMS Algorithm. *Electronics* **2023**, *12*, 2360. [[CrossRef](#)]
15. Garcia-Hernandez, M. A Variable-Step LMS-Based Adaptive Filtering Algorithm Using Standard Deviation. In Proceedings of the 2023 IEEE 9th International Workshop on Computational Advances in Multi-Sensor Adaptive Processing (CAMSAP), Los Sueños, Costa Rica, 10–13 December 2023; pp. 146–150.
16. Kwong, R.H.; Johnston, E.W. A Variable Step Size LMS Algorithm. *IEEE Trans. Signal Process.* **1992**, *40*, 1633–1642. [[CrossRef](#)]
17. United States Coast Guard (Ed.) *Loran-C User Handbook*; U.S. Government Printing Office: Washington, DC, USA, 1992; ISBN 978-0-16-041594-4.
18. United States Coast Guard. *Specification of the Transmitted Loran-C Signal—International Loran*; U.S. Department of Transportation: Washington, DC, USA, 1981.
19. Arutaki, A.; Chiba, J. Communication in a Three-Layered Conducting Media with a Vertical Magnetic Dipole. *IEEE Trans. Antennas Propag.* **1980**, *28*, 551–556. [[CrossRef](#)]
20. Shaw, A.; Al-Shamma'a, A.; Wylie, S.R.; Toal, D. Experimental Investigations of Electromagnetic Wave Propagation in Seawater. In Proceedings of the 2006 European Microwave Conference, Manchester, UK, 10–15 September 2006; pp. 572–575.

Disclaimer/Publisher's Note: The statements, opinions and data contained in all publications are solely those of the individual author(s) and contributor(s) and not of MDPI and/or the editor(s). MDPI and/or the editor(s) disclaim responsibility for any injury to people or property resulting from any ideas, methods, instructions or products referred to in the content.